



Nuclear Materials Authority  
P.O.Box 530 Maadi, Cairo, Egypt

DOAJ DIRECTORY OF  
OPEN ACCESS  
JOURNALS

ISSN 2314-5609  
Nuclear Sciences Scientific Journal  
9, 103- 118  
2020  
<http://www.ssnma.com>

## LINEAMENTS PATTERNS AND MINERALIZATION RELATED TO ALTERATION ZONES UTILIZING LANDSAT 8 SATELLITE IMAGERY FOR KADABORA AREA, CENTRAL EASTERN DESERT, EGYPT

MEDHAT I. A. MOUSA and GEHAD M. R. MANSOUR  
*Nuclear Materials Authority, Cairo, Egypt*

### ABSTRACT

The aim of this study is to mapping lineaments at the Kadabora granitic area, for a purpose of developing strategies and reconsider the relationship between the structural lineaments, radioactivity and alteration zones. The work deals with the relationship between the structure of lineaments and radioactivity in the study area. Image processing and statistical analysis of the obtained lineaments was performed and show ascendancy of NW-SE and NE-SW directions with 300457 m. in length of 503 lines of 43.7% and 251900 m. in length of 421 lines of 36.6% of the overall total of linear structures, respectively. Also, the North-South trend has about 126357 m. for 171 lines of 14.8%, but the E-W trend has about 27589 m. in length of 56 lines of 4.8%. These lineaments are totalizing 1151 segments and a global length of 706305 m. Results obtained join the main directions of digitized faults from the published geological map of the region, totalizing a length of 22625 m. There are three main anomaly zones for ratio image cover the study area, where Landsat 8 ratio image of band 4/2 shows alterations of ferruginous minerals. While, the image 5/6 gives alterations of ferromagnesian minerals and finally the ratio image 6/7 gives alterations of hydroxide-bearing minerals. The interpretation and analysis for radioactive anomaly and alteration zones and also the fracture frequency (length and number), explained that high radioactive locations occur in monzogranitic rocks which have high fracture density. On the other hand, the low radioactive zones occur within the syenogranitic as well as other country rocks which have a low fracture density in the study area.

### INTRODUCTION

The study area is situated in the Central Eastern Desert of Egypt between lat. 25°34'N and 25°26'N and long. 34°20' and 34°34'E and covers about 604 km<sup>2</sup> (Fig. 1). The investigated area is mostly composed of granitic pluton associated with large outcrops of metamorphic rocks. Its special importance is due to the fact that Kadabora granitic rocks contain a significant amount of radioactive mineralizations. The granites show different

structural trends which have been interpreted from a Landsat image.

The concept of lineament extraction (i.e. the mappable structures of linear or curvilinear shapes detected on earth surface) from digital satellite images can represent faults, valleys, soil tonal changes, straight streams or any line weakness that has been treated by several authors (Podwysoccki et al., 1975; Burdick and Speirer, 1980; Baumgartner et al., 1999; Mostafa and Bishta, 2004 and Bishta et al., 2010).

Lineament map has been constructed and correlated with radiometric maps of the same area. Various methods are used for lineament extraction; visual interpretation and manual digitizing techniques and automatic extraction using software and algorithms. The mapping of lineaments is a common method for the identification of faults and joints where detection and localization of faults are one of the most used criteria in geological investigations. From this perspective, the extraction of lineaments in the study area was studied in order to make a multi-criteria decision for the reconsider the relationship between the structural lineaments and radioactive elements. Kadabora Granitic Pluton has been investigated through several studies dealing with its magma source, mineralogy, radioactivity and physical dressing (i.e. El Ramly and Akaad, 1960; Kabesh et al., 1980; Ashmawy, 1993; El

Mahallawi and Molnar, 1994; El Sayed, 1998; Abu El Ela and Salem, 1999 and Ahmed, 2002).

The processing of satellite images involved composite of different images using various band triplets. Colour composites such as bands 7, 5 and 3 in RGB were prepared (Fig. 1). The fracture lineaments have been interpreted using directional filter technique.

The present study aims to; firstly mapping the different granitic phases of Kadabora Pluton and delineate structural trends that control the distribution of the mineralized zones in the area. Secondly, delineation and mapping alteration zones related to radioactive mineralization in Kadabora, using integrated remote sensing datasets (OLI image data) and airborne gamma ray spectrometer data with the previous field investigation.

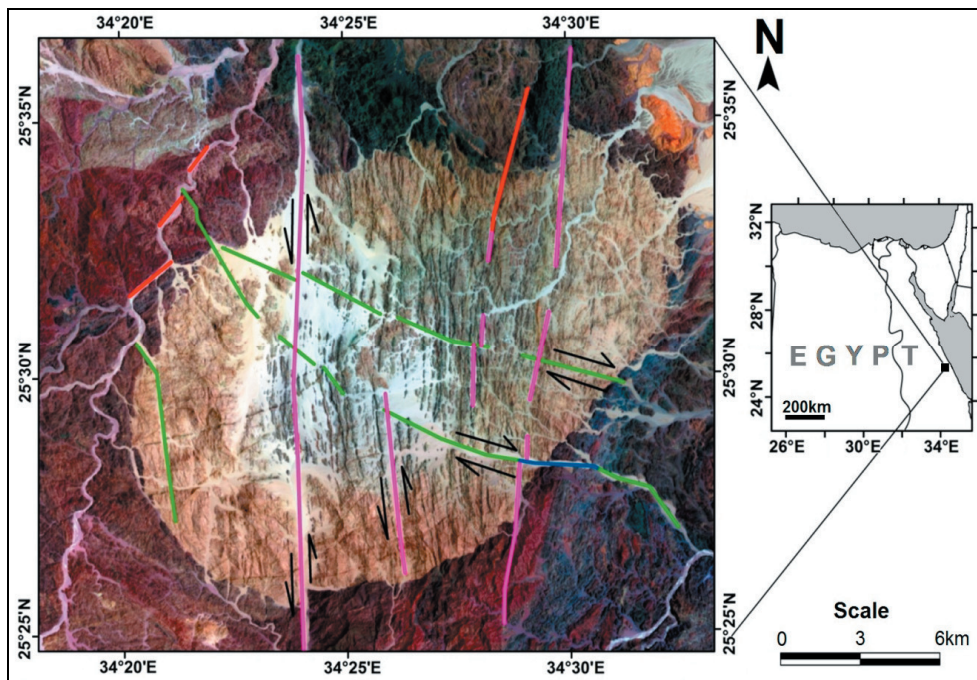


Fig. 1: False colour map shows location, major faults and wadis of the study area

Lineament map has been constructed and correlated with radiometric maps of the same area. Various methods are used for lineament extraction; visual interpretation and manual digitizing techniques and automatic extraction using software and algorithms. The mapping of lineaments is a common method for the identification of faults and joints where detection and localization of faults are one of the most used criteria in geological investigations. From this perspective, the extraction of lineaments in the study area was studied in order to make a multi-criteria decision for the reconsider the relationship between the structural lineaments and radioactive elements. Kadabora Granitic Pluton has been investigated through several studies dealing with its magma source, mineralogy, radioactivity and physical dressing (i.e. El Ramly and Akaad, 1960; Kabesh et al., 1980; Ashmawy, 1993; El Mahallawi and Molnar, 1994; El Sayed, 1998; Abu El Ela and Salem, 1999 and Ahmed, 2002).

The processing of satellite images involved composite of different images using various band triplets. Colour composites such as bands 7, 5 and 3 in RGB were prepared (Fig. 1). The fracture lineaments have been interpreted using directional filter technique.

The present study aims to; firstly mapping the different granitic phases of Kadabora Pluton and delineate structural trends that control the distribution of the mineralized zones in the area. Secondly, delineation and mapping alteration zones related to radioactive mineralization in Kadabora, using integrated remote sensing datasets (OLI image data) and airborne gamma ray spectrometer data with the previous field investigation.

**MATERIAL AND METHODS**

**Software**

Several types of software have been used (ERDAS IMAGINE, ENVI V. 5.1, PCI, and ARCGIS V. 10.2) for processing and analysis of multi-spectral and single band images. ARCGIS was used to georeference, digitize and capture various maps in a database.

**Data Acquisition and Preprocessing of Landsat 8 Image Data**

A Landsat 8 images with path 174 and a row 42, which acquired by the Operational Land Imager (OLI) on 9<sup>th</sup> June 2014. These images have been successfully used for

Table 1: Landsat 8 OLI and TIRS Spectral Bands.

<b>Bands</b>	<b>Band name</b>	<b>Instrument</b>	<b>Wavelength (µm)</b>	<b>Resolution</b>
<b>1</b>	<b>Coastal aerosol (blue)</b>	<b>OLI</b>	<b>0.433–0.453</b>	<b>30 m</b>
<b>2</b>	<b>Blue</b>	<b>OLI</b>	<b>0.450–0.515</b>	<b>30 m</b>
<b>3</b>	<b>Green</b>	<b>OLI</b>	<b>0.525–0.600</b>	<b>30 m</b>
<b>4</b>	<b>Red</b>	<b>OLI</b>	<b>0.630–0.680</b>	<b>30 m</b>
<b>5</b>	<b>Near Infrared (NIR)</b>	<b>OLI</b>	<b>0.845–0.885</b>	<b>30 m</b>
<b>6</b>	<b>Shortwave Infrared (SWIR) 1</b>	<b>OLI</b>	<b>1.560–1.660</b>	<b>30 m</b>
<b>7</b>	<b>Shortwave Infrared (SWIR) 2</b>	<b>OLI</b>	<b>2.100–2.300</b>	<b>30 m</b>
<b>8</b>	<b>Panchromatic</b>	<b>OLI</b>	<b>0.500–0.680</b>	<b>15 m</b>
<b>9</b>	<b>Cirrus</b>	<b>OLI</b>	<b>1.360–1.390</b>	<b>30 m</b>
<b>10</b>	<b>Thermal Infrared (TIRS) 1</b>	<b>TIRS</b>	<b>10.6-11.2</b>	<b>100 m</b>
<b>11</b>	<b>Thermal Infrared (TIRS) 2</b>	<b>TIRS</b>	<b>11.5-12.5</b>	<b>100 m</b>

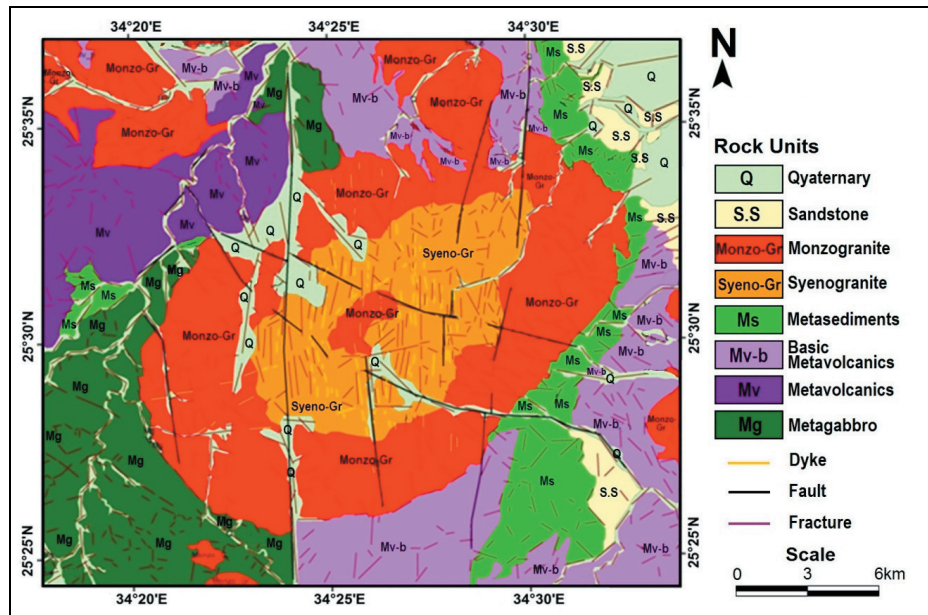


Fig. 2: Geologic map of Kadabora Pluton, Central Eastern Desert, Egypt

hydrothermal alteration mineral mapping in well-exposed areas. A Landsat 8 image of the area is the main data used for this study, which possess structural features which are commonly the expression of faults, fractures, and lithological boundaries. Lineament map is considered as a very important issue in different disciplines to solve certain problems with the area for mineral exploration. The classification of lineaments and its direction and length can be easily demarcated using satellite image. A wide variety of digital image processing technique was applied to classify the various geological rocks, and structural features of the area which delineates the associated alteration zones in the study area. The characteristic features of OLI images are shown in Table 1.

A scanned geological map of Egypt compiled by (Conoco, 1987) for the studied region with a scale of 1:500000 used to allow the comparison of the resulted lineaments with

the published map.

### Geologic Setting

Kadabora Granitic Pluton is oval-like shape with a NE-SW long extent of about 22 km, and NW-SE short extent of about 16 km, it shows high relief and sharp contact with the country rocks. Kadabora area has different lithologic units, including dyke swarms, granitoids, volcanogenic metasediments, metavolcanics (Mv), metasediments (Ms) and metagabbros (Mg) (Fig. 2). Kadabora represents a post tectonic zoned pluton consisting of monzogranites (Monzo-Gr) with only subordinate syenogranites (Syeno-Gr) that show potassic character with scarce sodic tendencies (Ahmed, 2002). About 23 pegmatite bodies are found in Kadabora Pluton that can be classified into two groups: The first one composed from quartz-feldspar-mica and the second one composed of quartz-feldspar.

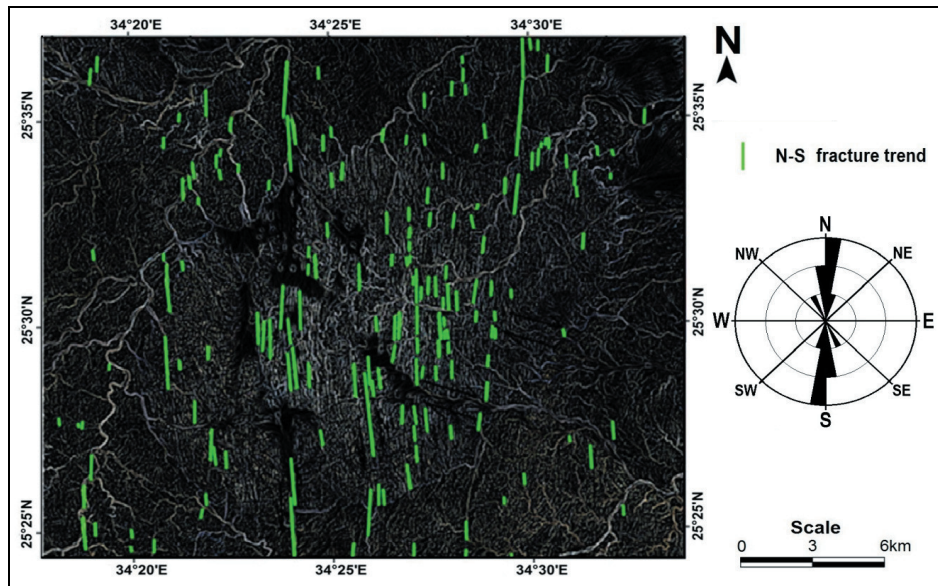


Fig. 3: Edge detection image shows lineaments of the N-S direction and their rose diagram

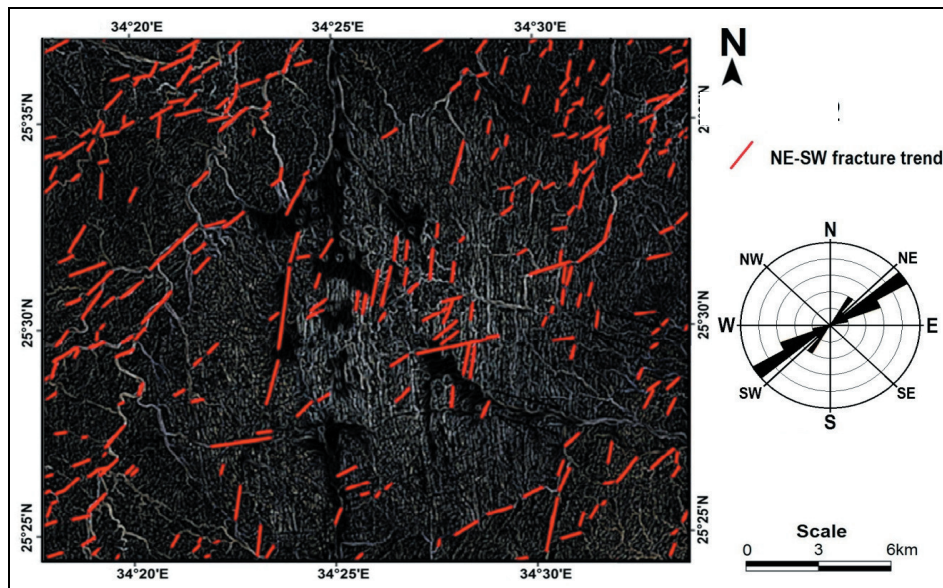


Fig. 4: Edge detection image shows lineaments of the NE-SW direction and their rose diagram

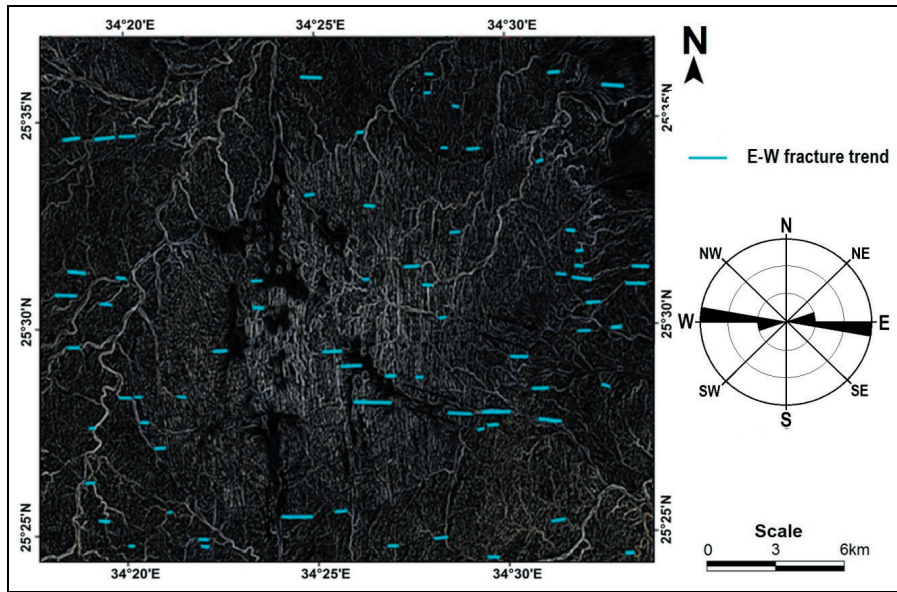


Fig. 5: Edge detection image shows lineaments of the E-W direction and their rose diagram

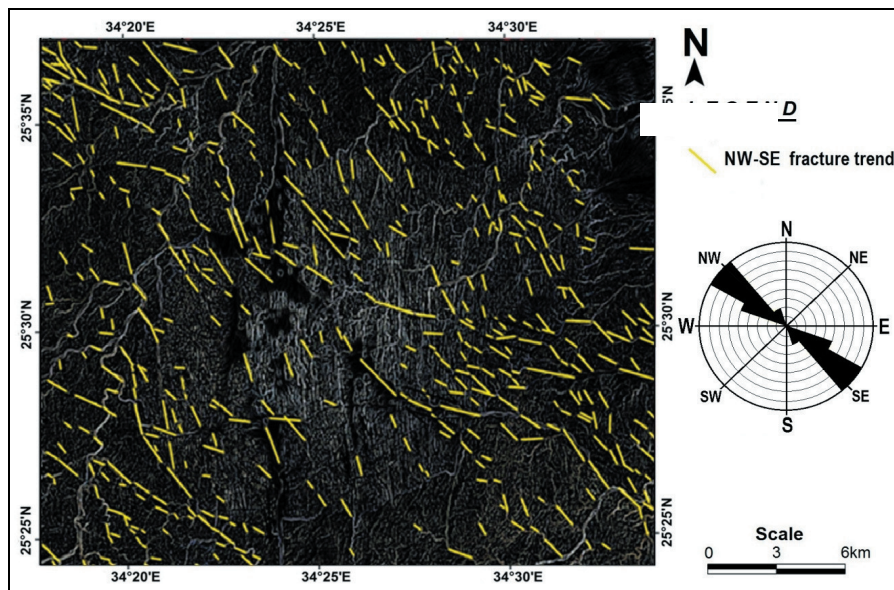


Fig. 6: Edge detection image shows lineaments of the NW-SE direction and their rose diagram

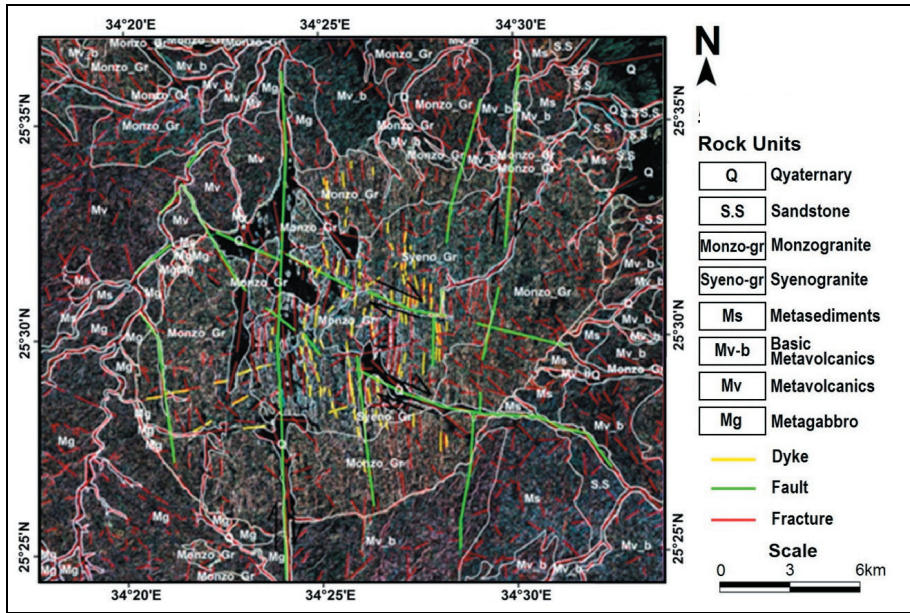


Fig. 7: Directional filter image shows all lineaments for Kadabara Pluton

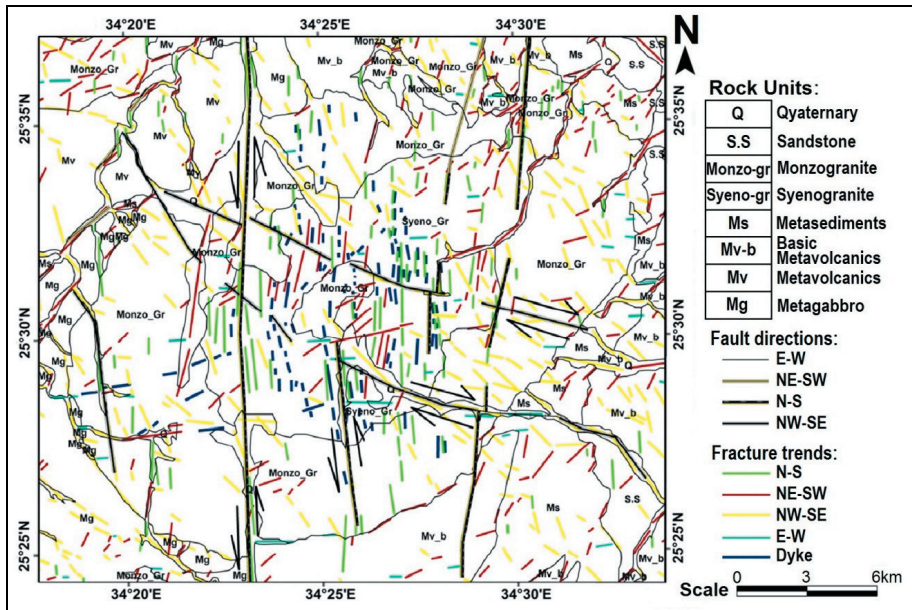


Fig. 8: Detailed geological map of Kadabara Pluton

The lithology of Kadabora area contains different lithologic units are listed from younger to older, including recent sediments, granitoids, metavolcanics, metasediments and metagabbros as well as dyke swarms and faults (Fig. 2).

### Directional Filters

Automatic lineament extraction in this study is performed by the directional filter of ENVI V. 5 and ARCGIS V. 10.2 software, respectively. The image enhancement is one of the useful tools to improve the interpretability. One of those enhancements is an edge sharpening enhancement technique for enhancing the edges in an image. Directionality filters (edge detection filters) are designed with enhanced linear features; the filters can be designed to enhance features which are oriented in specific directions. The filtering operation will sharpen the boundary that exists between neighbor units. Obtained the best results are shown on Figs. (3-7).

A remotely sensed lineament map was produced depending on directional filters and edge enhancement, which have N-S, E-W, NE-SW and NW-SE directions which plotted on Figure (7). The comparison between directional filter image and the detailed geological maps of Kadabora Pluton (Figs. 7 and 8), we note that most dykes of 45 km length are present in syenogranitic rocks (Syeno-gr) that have about an area 68 km<sup>2</sup> but, while most of structural lineaments present in monzogranite (i.e. alkali feldspar granite) which has an area about 193 km<sup>2</sup>. The orientation of lineaments showing major trends in NW-SE and NE-SW directions in this area, where fractures and faults acts as an apertures to flow of fertile flu-

ids that are rich in mineralizations. The precision of lineament map is calculated by using Arc GIS overlay technique where the lineaments and faults are matched.

### Alteration Zones

The present study will rely largely on the interpretation of Landsat 8 OLI image, whereby the fracture lineaments can be accurately mapped utilizing the band combination and directional filters. The rationing techniques were used to emphasize alteration zones.

Ratio images are known for enhancement of spectral contrasts among the bands considered in the rationing and have successfully been used in mapping alteration zones (Segal, 1983 and Kenea, 1997). The band rationing technique proved powerful in discriminating rocks rich in iron oxides and hydroxide minerals from the rest of the country rocks. Sabins (1999) explained how the TM ratio 5/7 distinguishes altered rocks containing clays and alunite from unaltered rocks, and how TM ratio 3/1 distinguishes altered rocks containing iron oxide. Ramadan et al. (2001) combined TM ratios 5/7, 4/5, 3/1 in red, green, and blue, respectively, to show alteration zones. Kaufmann (1988) studied the alteration minerals using ratio combinations of Landsat 8 (OLI) where ratio combinations using bands 7, 4, 3 and 5 in Landsat TM, is equivalent to bands 7, 5, 4 and 6 in Landsat 8 and ratio 7/4, 4/3 and 5/7 thus corresponds to ratio 7/5, 5/4 and 6/7 using Landsat 8, which revealed result such as clay minerals containing water (bound or unbound) micas, carbonates and hydrates are enhanced by band ratio 6/7 (5/7 in TM). On the other hand, the ferric and ferrous iron is best enhanced by band ratio 7/5 (7/4 in TM)

Table 2: Basic Statistics for all band ratios

Ratio	Minimum	Maximum	Mean	SD	Threshold Value
<b>B4/B5</b>	<b>1</b>	<b>255</b>	<b>105</b>	<b>65</b>	<b>170</b>
<b>B5/B6</b>	<b>0</b>	<b>255</b>	<b>102</b>	<b>56</b>	<b>158</b>
<b>B6/B7</b>	<b>0</b>	<b>255</b>	<b>130</b>	<b>58</b>	<b>188</b>

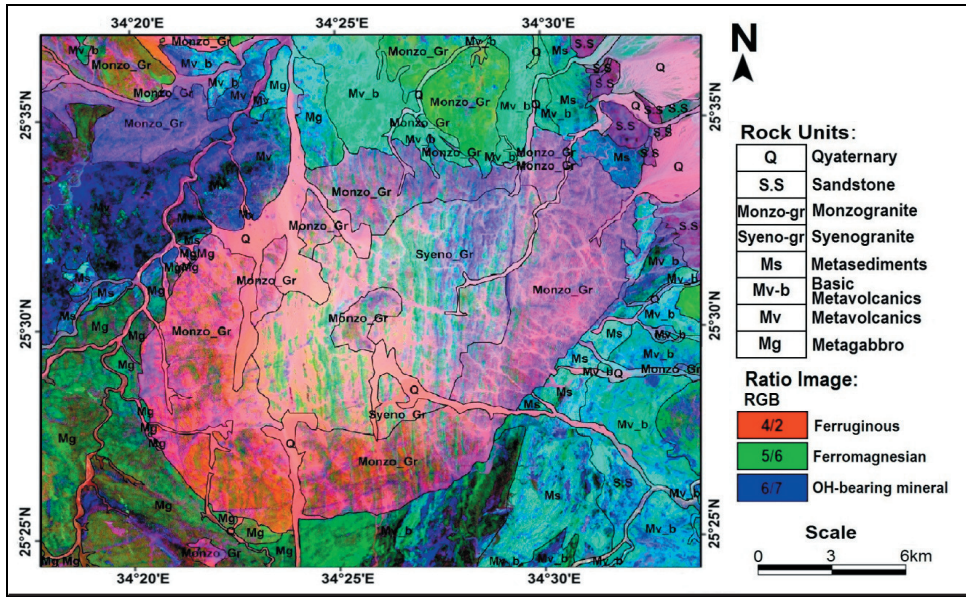


Fig. 9: Coloured ratio image compiled from 4/2, 5/6 and 6/7 band ratios in RGB

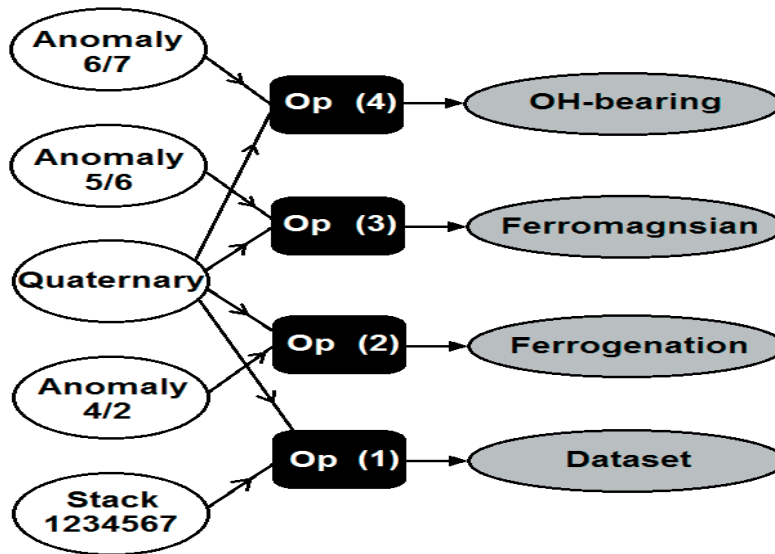


Fig. 10: Data model for alteration zones

due to major electronic transition bands in NIR (at  $\sim 0.87 \mu\text{m}$ ) and the visible charge transfer bands in the ultraviolet and unaffected SWIR range (Kaufmann, 1988).

The composite colour image created by band ratio 7/5, 5/4 and 6/7 (7/4, 4/3 and 5/7 in TM) displayed as RGB, results in an image which shows the red colour represents minerals containing iron ions, green represent vegetated zones and blue represent  $\text{OH}/\text{H}_2\text{O}$ ,  $\text{SO}_4^-$  or CO-bearing minerals (Kaufmann, 1988). Here the OLI was designed to detect the assemblages of alteration minerals (iron oxides, clay, and alunite) that occur in altered rocks where it's an earlier Landsat instrument. Using the theoretical knowledge about the spectral properties of most rocks and minerals, Landsat 8, OLI images of 4/2 and 5/6 were selected for ferruginous and ferromagnesian rocks respectively but 6/7 for hydroxyl bearing minerals. Based on the above considerations, there are ratios colour composite images using combinations of bands 4/2, 5/6 and 6/7 in R, G and B, respectively. We can

construct several steps for rationing method using ENVI software were band ratio images such as band 4/2, 5/6 and 6/7 in gray scale and all ratio images stacked together respectively in order to obtain colour composite image in RGB (Fig. 9).

Basic Statistics for all band ratios were given in Table 2, where Threshold Value indicates the result from all statistics to construct alteration zones images using ENVI software.

We can compute basic Statistics for all band ratios which given in Table 2. All steps for construction of alteration zones image given by data model represented on Figure (10), and finally three images for alteration zones which grouped together to give one coloured ratio image shows alteration zones in the study area.

Then we can construct anomalous zones for each ratio image. Ratio image 4/2 give alterations of ferruginous minerals, ratio image 5/6 give alterations of ferromagnesian minerals and finally ratio image 6/7 give al-

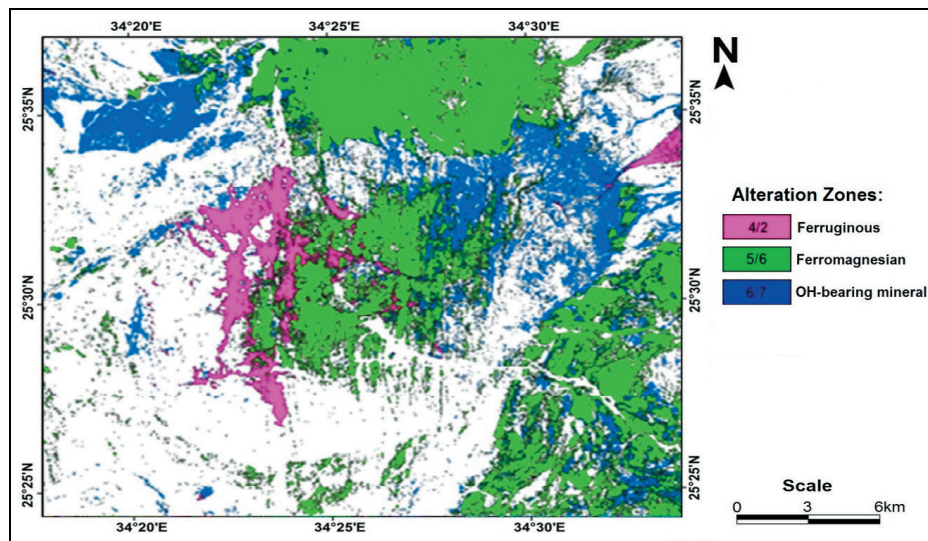


Fig. 11: Alteration zones in the study area (4/2 for ferruginous minerals, 5/6 for ferromagnesian and OH-bearing minerals)

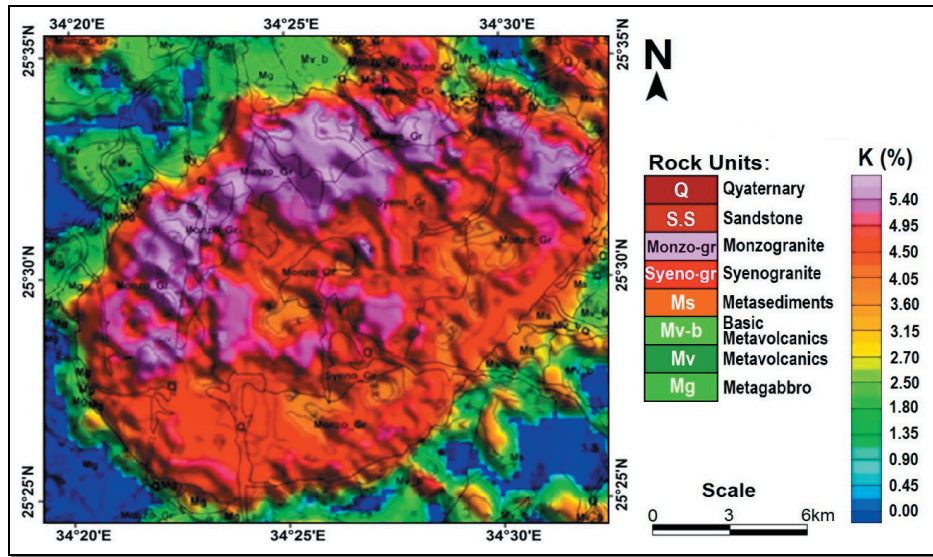


Fig. 12: Potassium (K %) shaded relief distribution map of Kadabora Pluton, Central Eastern Desert, Egypt (Modified after Aboelkhair et al., 2014)

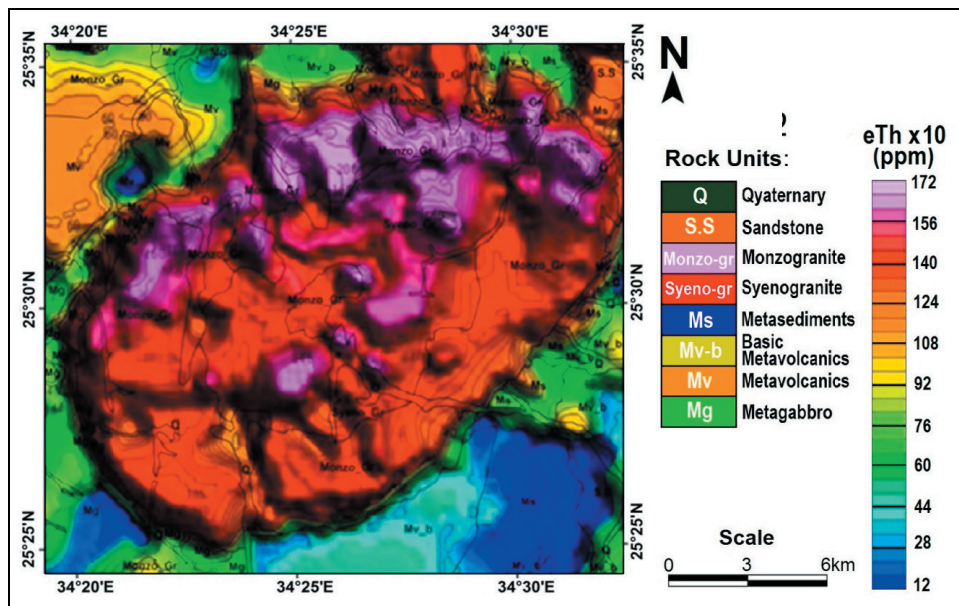


Fig. 13: Equivalent Thorium (eTh ppm x 10) shaded relief distribution map of Kadabora Pluton, Central Eastern Desert, Egypt (Modified after Aboelkhair et al., 2014)

terations of OH-bearing minerals as on Figure (11). Alterations of ferruginous zone are shown outside granitic pluton for Kadabora area which has a low density in fracture elements. The ferromagnesian alteration zone is given at syenogranite which has low fracture lineaments and high density in dykes. Finally, OH bearing mineral alteration zone is present in monzogranitic rocks which has a high density of fracture and low dykes.

#### Radioactivity of the Study Area

The granitic rocks of Kadabora may be regarded as homogeneous representing crystallization of the granitic magma in one phase of emplacement. Kadabora Pluton is characterized by higher concentrations of Th, U and K at its northern part.

#### Potassium

Potassium distribution was presented on Figure (12) and increase northwards over the whole pluton. Potassium contents range be-

tween 2 and 6%. Secondary potassium alteration zones in the northern part of the pluton are may be attributed to decrease of thorium to potassium ratios.

#### Thorium

Thorium is more resistant to environmental leaching processes than uranium. The equivalent thorium contour map (Fig. 13) subdivided Kadabora Pluton into three parts; the southern part located SW with a lower thorium concentration of about 11 ppm, the central part with medium concentration of about 14 ppm, and the northern part with higher concentrations of about 17 ppm. The central part of the pluton core is mainly monzogranite in composition while, the southern and the northern parts are mainly syenogranite exhibiting different Th concentrations. The southern part suffered from leaching of radioelements, while the northern part of the pluton has characteristic features that help in increasing the late magmatic thorium concentrations due to hydrothermal activity. The granitic rocks of

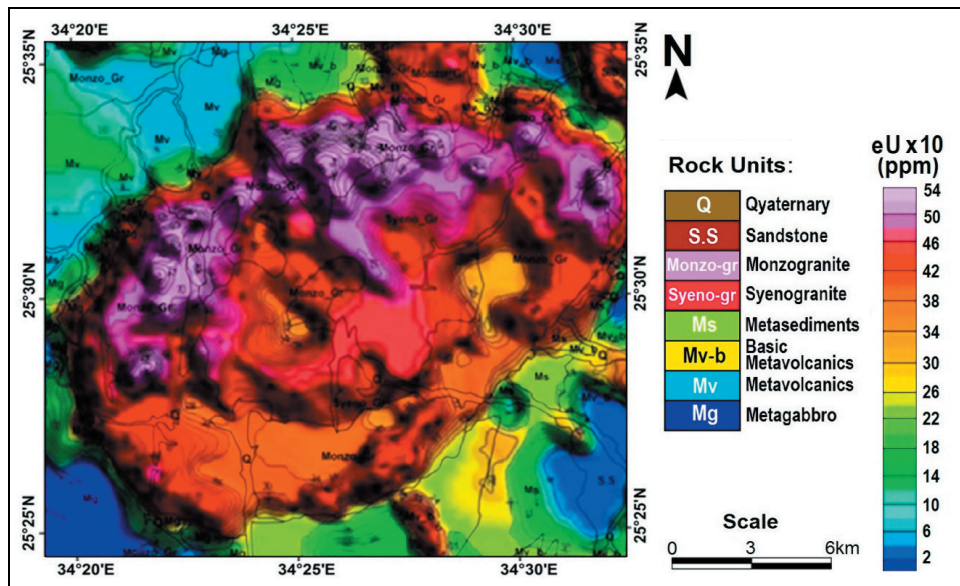


Fig. 14: Equivalent Uranium (eU ppm x 10) shaded relief distribution map of Kadabora Pluton, Central Eastern Desert, Egypt (Modified after Aboelkhair et al., 2014)

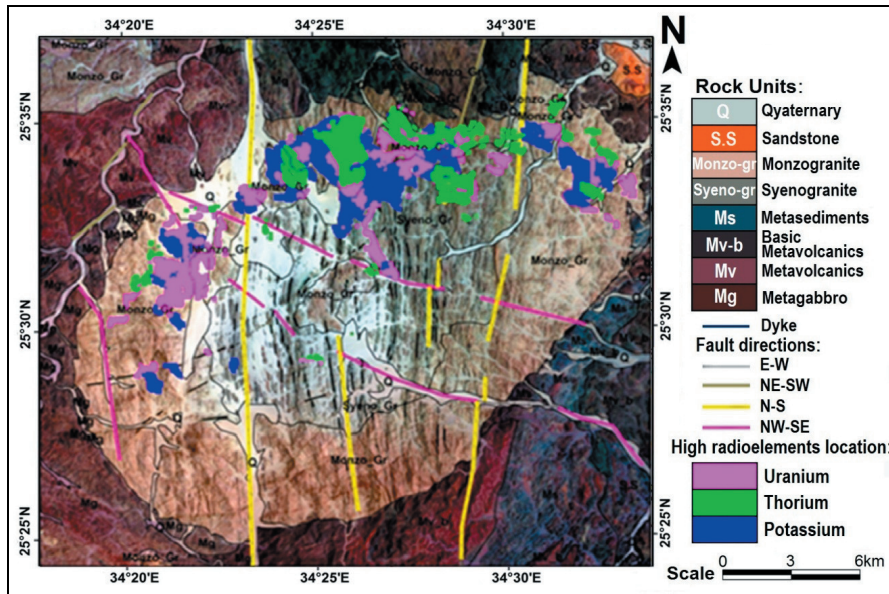


Fig. 15: High radioactive elements location map of Kadabora Pluton, Central Eastern Desert, Egypt

Kadabora may be regarded as homogeneous representing crystallization of the granitic magma in one phase of emplacement. So magma differentiation trend follows up is very easy from equivalent thorium distribution map, where the center of the pluton was crystallized first, followed with the outer part of the pluton and at the end pegmatite as late magmatic stage.

### Uranium

Uranium is a more mobile element than thorium, so if thorium is a very good indicator of the magmatic processes, uranium is a good indicator for the post-magmatic alteration processes. Kadabora Pluton can easily be subdivided into three parts the southern part with U-leaching, the central part with partly U-enrichment and the northern part with extensive U-enrichment. Pegmatite bodies, especially mineralized type are located in the outer part of the pluton. The U higher values are concentrated mainly in the northern outer parts of the

pluton more than in the central and southern parts with a maximum value of about 6 ppm as shown on Figure (14). Dyke swarms (Fig. 8) of different composition affect the uranium migration processes that clearly appear in the east of the studied area where uranium concentrations is very low. On the other hand, from Figure (14) we also note that the syenogranite shows more susceptible to leaching than monzogranite.

Integration of alteration zones and structural elements maps and radioactivity datasets give us idea about relations between the three datasets which are given on Figure (15). Construction of alteration maps in concise with structural lineament led to delineate favorable sites for uranium mineralization in Kadabora granites. From the dataset analysis, the syenogranites are not only enriched in magmatic radioelements, but they have the ability to host secondary mineralization, and show very higher response to leaching processes than other rocks like monzogranite. Figure (15) shows

Table 3: Relation between high radioactive elements and fracture density

Rock	Anomaly name	Area (km <sup>2</sup> )	Number of lineaments	Number (%)	Length of lineaments	Length (%)
Monzogranite + syenogranite	K	27.36	64	0.275862	50584.922654	0.298
Monzogranite + syenogranite	Th	27.50	78	0.336207	55883.35896	0.329
Monzogranite	U	41.59	90	0.387931	63252.536269	0.372

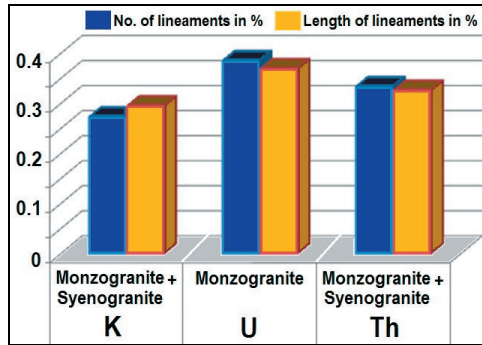


Fig. 16: Relation between rock types, fracture density and radioactivity in the study area

high radioelement's sites, which present at a high elevated portion of Kadabora Pluton and enriched in monzogranitic rocks which have a high structural elements and high ferruginous plus ferromansian bearing minerals.

Table (3) gives the relation between radioactive elements and fracture density, where potassium radioelement has an area about 27.36 km<sup>2</sup>, which has 64 structural lineaments of 50584 ms which presented at monzogranite. High Thorium content which has an area about 27.5 km<sup>2</sup> and presented in monzogranite and syenogranite has 78 fracture lineaments of length 55883 ms. Finally, high Uranium content present in monzogranite which has an area about 41.59 km<sup>2</sup> and 90 line of structural lineaments of an length 63252 m. Figure 16 gives us idea about representing relations between rock types and fracture density with radioactivity in the study area.

## SUMMARY AND CONCLUSION

Remote Sensing techniques are an efficient tool for geological mapping. We can delineate special location for rock units and high radioactive elements as well as fracture lineaments. We can find the relation between high radioactive zones and fracture frequency (number and length), where high radioactive location occurs in monzogranitic rocks which have a high fracture frequency in the study area. Lineaments extracted by a directional filter method. A statistical analysis of the lineament network based on their direction and length revealed a trend of two principal directions; NW-SE, followed by the NE-SW, the other directions proportions are E-W and N-S. Fractures and faults with more or less north-south direction help in the hydrothermal solution circulation, especially in the northern parts and controlled their redistribution. Remote Sensing used in mineral exploration of hydrothermal ore deposits often use the spectral reflectance for chemical composition of that rocks which represent minerals associated with it. Based on the spectral properties of typical alteration mineral and geological background, ratio image processing techniques were selected to recognize different alteration minerals. Based on the spectral properties of typical alteration mineral and geological background, ratio image processing techniques were selected to recognize different alteration minerals. Construction of alteration maps in concise with structural lineament led to delineate favorable sites for alteration mineralization in Kadabora granites. Kadabora Pluton can easily be subdivided into three parts, the southern part with

alteration-leaching, the central part with partly alteration-enrichment and the northern part with extensive alteration-enrichment. Image processing techniques were used to better distinguish Kadabora alteration zones, moreover ratio image and structural lineaments show the favorable relation between frequency and direction of lineaments and alteration zones. It indicated from detailed remote sensing and previous work that dike swarms help in radioelement's redistribution after remobilization, doleritic dykes to the east act as a seal in uranium migration, while acidic dikes to the center trapped the mineralization.

### REFERENCES

- Aboelkhair, H.; Hasan, E. and Sehsah, H., 2014. Mapping of structurally controlled Uranium mineralization in Kadabora granite, Central Eastern Desert, Egypt using remote sensing and gamma ray spectrometry data. *The Open Geol. J.*, 8, (Suppl 1: M4) 54-68.
- Abu El Ela, A.M. and Salem, I.A., 1999. Petrological and geochemical studies on the dyke swarms of the Kadabora granite pluton, Eastern Desert, Egypt. *Ann. Geol. Surv. Egypt. (XXII)*, 47-63.
- Ahmed, A.R., 2002. Geology, Petrography, Geochemistry and Radioactivity of Kadabora area, Central Eastern Desert of Egypt. Unpublished Ph.D. Thesis, South Valley Univ., Aswan.
- Ashmawy, M.H., 1993. Dike swarms and fracture pattern analyses of the Kadabora granite pluton, Eastern Desert, Egypt. *ITCJ*, 1, 88-97.
- Baumgartner, A.; Steger, C.; Mayer, H.; Eckstein, W. and Ebner, H., 1999. Automatic road extraction based on multi-scale, grouping and context. *Photo. Eng. and Rem. Sens.*, 65, 777-785.
- Bishta, A.Z.; Mohamed, A.; Soliyman, A.A.M. and Mohamed A.A., 2010. Utilization of lineaments extraction from satellite imageries in structural mapping and mineral exploration of central Wadi Araba, Southwest Jordan. *JKAU Earth Sci.*, 21(2), 1-27.
- Burdick, R.G. and Speirer, R.A., 1980. Development of a method to detect geologic faults and other linear features from Landsat images. U. S. Bureau of Mines Report Inv., 8413-8474.
- Conoco Coral Corporation and Egyptian General Petroleum Corporation, 1987. Geological map of Gabel Hamata.
- El Mahallawi, M.M. and Molnar, Z.S., 1994. REE Geochemistry of the Post Granite Dykes of Gabal Kadabora Area, central Eastern Desert, Egypt, *Egypt. Mineralogist*, 6, 141-52.
- El Ramly, M.F. and Akaad M.K., 1960. The basement complex in the Eastern Desert between Lat. 24°30' and 25°40'N. *Geol. Surv. Egypt*, paper No. 8.
- El Sayed, M.M., 1998. Tectonic setting and petrogenesis of the Kadabora pluton: a late Proterozoic anorogenic A-type younger granitoid in the Egyptian Shield. *Chem De Erde-Geochem*, 58, 38-63.
- Kabesh, M.L.; Hilmy, M.E. and Salem, A.K.A., 1980. Behavior of major elements in the granitic rocks of Kadabora Pluton, Eastern Desert, Egypt. *Acta Mineral. Petrogr. Szeged. XXIV/2*, 245-56.
- Kaufmann, H., 1988. Concepts, processing and results. *Intern. J. Rem. Sens.*, 9(10-11), 1639-1658.
- Kenea, N.H., 1997. Digital Enhancement of Landsat Data, Spectral Analysis and GIS Data Integration for Geological Studies of the Derudeb Area, southern Red Sea Hills, NE Sudan, *Berliner Geowiss. Abh.*, D 14, Berlin. 116 p.
- Mostafa, M.E. and Bishta, A.Z., 2004. Significance of lineament patterns in rock unit classification and designation: a pilot study on Gharib-Dara area, northern Eastern Desert, Egypt. *Intern. J. Rem. Sens.*, 25, 1-13.
- Podwysocki, M.H.; Moik, J.G., and Shoup, W.D., 1975. Quantification of Geologic Lineaments by Manual and Machine Processing Techniques. *Proc. NASA Earth Resources Survey*

- Symposium, Houston, Texas, 885 -903.
- Ramadan, T.M.; Abdelsalam, M.G., Stern, R.J., 2001. Mapping Gold-Bearing Massive Sulfide Deposits in the Neoproterozoic Allaqi Suture, Southeast Egypt with Landsat TM and SIR-C/X SAR Images. Photo. Eng. and Rem. Sens., 67(4), 491-497.
- Sabins, F.F., 1999. Remote Sensing for Mineral Exploration. Ore Geol. Rev., 14, 157-183.
- Segal, D.B., 1983. Use of Landsat Multispectral Scanner Data for Definition of Limonitic Exposures in Heavily Vegetated Areas. Econ. Geol., 78, 711-722.

## الأنماط الخطية والتمعدنات المرتبطة بمناطق التغيرات باستخدام صور الأقمار الصناعية لاندسات ٨ لمنطقة كادابورا، وسط الصحراء الشرقية، مصر

مدحت إسماعيل أحمد موسى و جهاد محمد رضا منصور

تهدف هذه الدراسة إلى رسم خطوط التراكيب الجيولوجية لكتلة الجرانيت بمنطقة كادابورا مما يمكن من وضع الإستراتيجيات لإعادة النظر في العلاقة بين الخطوط التركيبية ومناطق التغيرات المتعلقة بالعناصر المشعة، حيث تم إجراء معالجة للصور الفضائية والتحليل الإحصائي للخطوط الناتجة وإستعراض الإتجاهات من نوع شمال غرب - جنوب شرق وشمال شرق - جنوب غرب بطول إجمالي قدره ٣٠٠٤٥٧ متراً لعدد ٥٠٣ خط بنسبة قدرها ٤٣,٧٪ و ٢٥١٩٠٠ متراً لعدد ٤٢١ خط بنسبة ٣٦,٦٪ على التوالي من المجموع الكلي للخطوط التركيبية، في حين حاز الإتجاه الشمالي - الجنوبي على ١٢٦٣٥٧ متراً لعدد ١٧١ خط بنسبة ١٤,٨٪، والإتجاه الشرقي - الغربي على ٢٧٥٨٩ متراً لعدد ٥٦ من التراكيب الخطية أي بنسبة ٤,٨٪. هذه الخطوط في مجموعها حوالي ١١٥١ خط بطول إجمالي حوالي ٧٠٦٣٠٥ متراً. أما الإتجاهات الرئيسية فيبلغ مجموعها ٢٢٦٢٥ متراً، وقد بينت الدراسة أن مناطق الشاذات الإشعاعية تتناسب مع عدد الخطوط التركيبية للمنطقة، حيث أعطت المرئيات ذات النسبة ٤/٢ أماكن التغيرات لصخور معادن الحديد. بينما مرئية النسبة ٥/٦ أظهرت أماكن التغيرات للصخور الحاملة على معادن الحديد والماغنسيوم وأخيراً مرئية النسبة ٦/٧ أوضحت أماكن التغيرات للصخور الحاملة على معادن الهيدروكسيدات. كما أوضح تحليل وتفسير المناطق المشعة ومناطق التغيرات وكثافة الكسور من حيث العدد والطول في منطقة الدراسة أن أعلى المناطق إشعاعياً تقع في صخور المونوزجرانيت والتي تتسم بكثافة عالية للكسور بينما الأماكن المنخفضة في التمدنات المشعة تقع في صخور السيانوجرانيت والتي تتسم بكثافة منخفضة للكسور.